# Experiment #2: AIRFOIL PRESSURE DISTRIBUTION
# AE 460: Aerodynamics & Propulsion Laboratory

Talbot Lab Room 18D (Basement)
Department of Aerospace Engineering
University of Illinois at Urbana-Champaign

**Full Laboratory Report Format due 1 week after completing the laboratory**

9/14 – 9/18 Group A conducts Laboratory 2 during the first hour of the lab session
Group B conducts Laboratory 2 during the second hour of the lab session

**SAFETY**

1. Eye protection should be worn at all times while the wind tunnel is being used. The fan can be very noisy so ear protection is also provided.
2. For the same reason, make sure that there are no loose papers on tables or chairs.
3. Wait for the Teaching Assistant to turn on the wind-tunnel main power before beginning the experiment.
4. Stay out of the path of the entrance and exit of the tunnel.
5. Everyone must have building access granted in the Safer Illinois app in order to enter the laboratory.
6. Wipe down shared equipment before and after use with sanitizing wipes.

## 1. OBJECTIVES

The purpose of this experiment is to measure and analyze the pressure distribution about an airfoil mounted in a wind tunnel. Pressure measurements obtained from the static pressure ring and the calibration coefficient calculated from the Tunnel Calibration Experiment will be used to determine the test-section airspeed. Pressures will be measured on the upper and lower surfaces of a Clark Y14 airfoil model at various angles of attack. The pressure distribution will be used to calculate the airfoil lift and moment coefficients. Additionally, flow visualization using tufts will be utilized to qualitatively describe the flow near the surface and areas of recirculation and separation.

## 2. BACKGROUND

Determining the airfoil pressure distribution is an important way to study the performance characteristics of an airfoil profile. Wind tunnel experiments on scale models are often used to verify the design of airfoil sections for large aircraft. These tests can save money by improving the design before a full-scale prototype is built. Experimental testing is also used to verify the results of numerical airfoil-performance codes.

## 2.1. Pressure Distribution

The conventional way of presenting pressure distribution data is in the form of the non-dimensional pressure parameter called the pressure coefficient, i.e.,

$$C_p = \frac{p_{measured} - p_\infty}{\frac{1}{2}\rho_\infty V_\infty^2} = \frac{p_{measured} - p_\infty}{q_\infty} = \frac{\Delta p_{measured}}{q_\infty} \tag{1}$$

where in the present case,

$p_{measured}$ = static pressure on the model surface [lbf/ft$^2$; N/m$^2$]
$p_\infty$ = freestream pressure [lbf/ft$^2$; N/m$^2$]
= test-section static pressure
$\rho_\infty$ = density of air [slug/ft$^3$; kg/m$^3$]
$V_\infty$ = freestream velocity [ft/sec; m/sec]
= test-section airspeed
$q_\infty$ = freestream dynamic pressure [lbf/ft$^2$; N/m$^2$]
$\Delta p_{measured}$ = static differential pressure on the model surface as measured in the experiment [lbf/ft$^2$; N/m$^2$]

Note that $\Delta p_{measured}$ as measured in the experiment is the differential pressure defined by the quantity ($p_{measured} - p_\infty$), since the reference pressure port will be connected to the wind tunnel static pressure ring.

Figure 1 shows a typical pressure distribution on a lifting airfoil. The pressure coefficients are plotted versus the chordwise position on the airfoil surface and are represented by the curved solid lines. Most of the upper-surface values are negative, and it is traditional to plot the negative pressures in the upward direction of the graph's *y*-axis. The pressure coefficient equals unity at the stagnation point on the airfoil. The integration over the upper and lower surface pressures indicates the amount of lift produced by the airfoil.

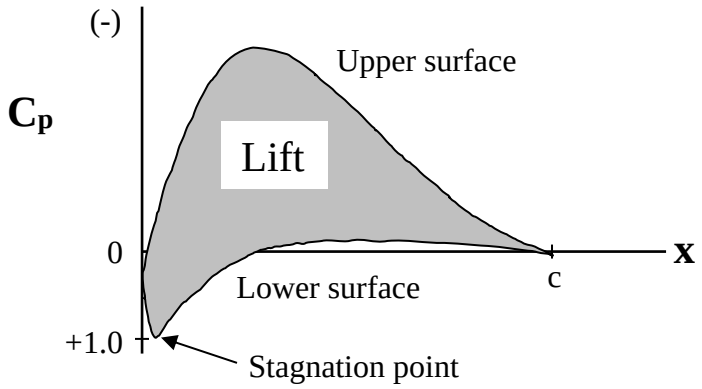


**Figure 1. Typical pressure distribution on an airfoil producing lift.**

## 2.2. Normal and Axial Force Components

The distribution of pressure that acts on the airfoil surface is often analyzed to calculate the forces exerted on the airfoil. These forces are often considered in the normal and axial directions. The normal direction is perpendicular to the airfoil chord line, and the axial direction is parallel to

the airfoil chord line. The normal and axial force components can then be used to calculate the lift force and the drag force due to pressure on the airfoil surface.

The pressure acting on the airfoil surface is illustrated in Figure 2 with the normal (*N*) and axial (*A*) axis directions shown (note that the image is of a symmetrical airfoil for illustrative purposes, while we will use a Clark Y14 airfoil in this lab). Four quadrants have been identified for which the normal and axial force components will be calculated. The pressure always acts perpendicular and onto the airfoil surface. The pressure acting on the upper airfoil surface is $p_u$, and the pressure acting on the lower surface is $p_l$. The angle between the pressure direction and the normal direction is defined as θ. This angle is positive when measured clockwise from the normal to the pressure direction, and negative when measured counterclockwise.

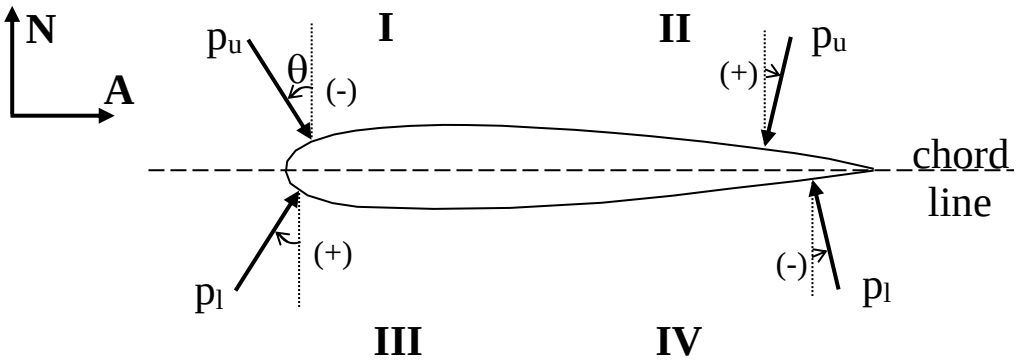


**Figure 2. The direction of the normal and axial forces and direction the pressure acts on an airfoil.**

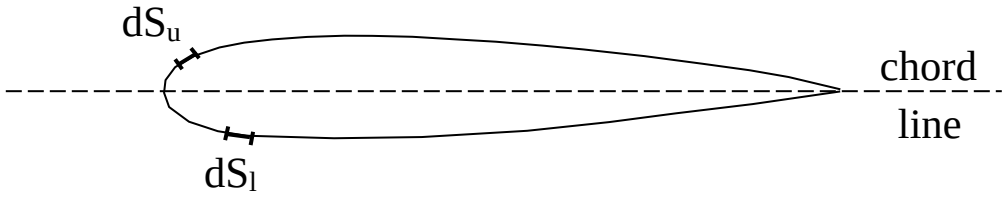


**Figure 3. Upper and lower elemental areas as defined on the airfoil.**

A force is defined as pressure acting over an area. Figure 3 shows two elemental surface areas; the upper surface element is $dS_u$, and the lower surface element is $dS_l$. The force per unit span acting on element $dS$ is $dF' = pdS$. Note that the prime denotes per unit span. The component of this force acting in the normal direction is $dN' = dF' \cos\theta = p \cos\theta \, dS$. Similarly, the component of this force acting in the axial direction is $dA' = dF' \sin\theta = p \sin\theta \, dS$. Dividing these parameters into the four quadrants presented earlier facilitates determination of the force equations. The parameters are listed in Table 1 with the corresponding positive or negative sign associated with each. The signs of the force components are dictated by the direction of the pressures.

**Table 1. Signs of parameters used to calculate the forces for various quadrants on the airfoil.**

| Quadrant | Pressure | N' | A' | θ | cosθ | sinθ |
|---|---|---|---|---|---|---|
| I | $p_u$, ↘ | - | + | - | + | - |
| II | $p_u$, ↙ | - | - | + | + | + |
| III | $p_l$, ↗ | + | + | + | + | + |
| IV | $p_l$, ↖ | + | - | - | + | - |

In order to maintain the required signs established in Table 1, the equations for the differential normal and axial force components are as shown in Table 2.

**Table 2. Equations for the differential normal and axial force components in defined quadrants.**

| Quadrant | Normal Force Component | Axial Force Component |
|---|---|---|
| I | $dN_u' = -p_u \cos\theta \, dS_u$ | $dA_u' = -p_u \sin\theta \, dS_u$ |
| II | $dN_u' = -p_u \cos\theta \, dS_u$ | $dA_u' = -p_u \sin\theta \, dS_u$ |
| III | $dN_l' = p_l \cos\theta \, dS_l$ | $dA_l' = p_l \sin\theta \, dS_l$ |
| IV | $dN_l' = p_l \cos\theta \, dS_l$ | $dA_l' = p_l \sin\theta \, dS_l$ |

The differential elements are then summed up by integrating over the airfoil surface from the leading edge (LE) to the trailing edge (TE) in order to determine the total normal and axial force components as given by

$$N' = \int_{LE}^{TE} dN_u' + \int_{LE}^{TE} dN_l' = -\int_{LE}^{TE} p_u \cos\theta \, dS_u + \int_{LE}^{TE} p_l \cos\theta \, dS_l$$
$$A' = \int_{LE}^{TE} dA_u' + \int_{LE}^{TE} dA_l' = -\int_{LE}^{TE} p_u \sin\theta \, dS_u + \int_{LE}^{TE} p_l \sin\theta \, dS_l \qquad (2)$$

Note that these forces (and the moment presented in the following section) only include the pressure component. There is also a (small) skin-friction component that has been neglected in this analysis.

### 2.3. Moment About the Leading Edge

The moment about the airfoil leading edge can be calculated by considering the forces caused by the pressures acting on the surface. The sign convention for the moment is positive for a moment that causes the airfoil leading edge to rotate upward, and negative for a moment that causes the leading edge to rotate downward. Figure 4 illustrates the direction for positive moment and how it is calculated from the normal and axial forces.

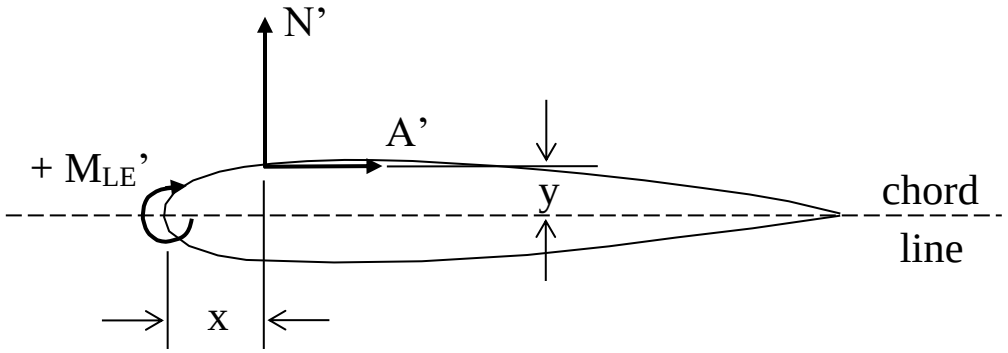


**Figure 4. Direction of a positive leading edge moment.**

The moment due to a normal force per unit span acting on *dS* is $dM_n' = p \cos\theta\, x\, dS$. Similarly, the moment due to an axial force per unit span acting on *dS* is $dM_a' = p \sin\theta\, y\, dS$. The parameters *x* and *y* are the moment arms from the normal and axial force components to the leading edge, respectively. The signs associated with each of the parameters used to calculate the moment are listed in the Table 3 given below.

**Table 3. Signs of parameters used to calculate the moment for various quadrants on the airfoil.**

| Quadrant | Pressure | $M_n'$ | $M_a'$ | x | y | θ | cosθ | sinθ |
|---|---|---|---|---|---|---|---|---|
| I | $p_u$, ↘ | + | + | + | + | - | + | - |
| II | $p_u$, ↙ | + | - | + | + | + | + | + |
| III | $p_l$, ↗ | - | - | + | - | + | + | + |
| IV | $p_l$, ↖ | - | + | + | - | - | + | - |

In order to maintain the required signs established above, the equations for the differential moments are given in Table 4.

**Table 4. Equations for the differential moments for normal and axial components for the quadrants on the airfoil.**

| Quadrant | Normal Moment Component | Axial Moment Component |
|---|---|---|
| I | $dM_n' = p_u \cos\theta\ x\ dS_u$ | $dM_a' = -p_u \sin\theta\ y\ dS_u$ |
| II | $dM_n' = p_u \cos\theta\ x\ dS_u$ | $dM_a' = -p_u \sin\theta\ y\ dS_u$ |
| III | $dM_n' = -p_l \cos\theta\ x\ dS_l$ | $dM_a' = p_l \sin\theta\ y\ dS_l$ |
| IV | $dM_n' = -p_l \cos\theta\ x\ dS_l$ | $dM_a' = p_l \sin\theta\ y\ dS_l$ |

The resulting moment per unit span about the airfoil leading edge determined by summing up the differential elements by integration is given as

$$M_{LE}' = \int_{LE}^{TE} dM_n' + \int_{LE}^{TE} dM_a' = \int_{LE}^{TE} (p_u \cos\theta\ x - p_u \sin\theta\ y) dS_u + \int_{LE}^{TE} (-p_l \cos\theta\ x + p_l \sin\theta\ y) dS_l \quad (3)$$

## 2.4. Normal, Axial and Moment Coefficients

Forces and moments are often considered in non-dimensional form. The normal force coefficient, axial force coefficient, and moment coefficient are the non-dimensional parameters corresponding to the forces and moments presented in the previous sections.

$$C_n = \frac{N'}{q_\infty c} \qquad C_a = \frac{A'}{q_\infty c} \qquad C_{m_{LE}} = \frac{M'_{LE}}{q_\infty c^2} \tag{4}$$

Substitution of the normal force integral equation into the above definition for $C_n$ yields

$$C_n = -\int_{LE}^{TE} \frac{p_u}{q_\infty} \cos\theta \; d\left(\frac{S_u}{c}\right) + \int_{LE}^{TE} \frac{p_l}{q_\infty} \cos\theta \; d\left(\frac{S_l}{c}\right) \tag{5}$$

where $c$ is the airfoil chord. However, $dS \cos\theta = dx$ resulting in

$$C_n = -\int_0^c \frac{p_u}{q_\infty} \; \frac{dx}{c} + \int_0^c \frac{p_l}{q_\infty} \; \frac{dx}{c} = \int_0^c \left( -\frac{p_u}{q_\infty} + \frac{p_l}{q_\infty} \right) \; \frac{dx}{c} \tag{6}$$

Manipulation of the equation allows the introduction of the pressure coefficient in the equation as is shown below.

**Normal force coefficient:**

$$C_n = \int_0^c \left( -\frac{p_u}{q_\infty} + \frac{p_l}{q_\infty} + \frac{p_\infty}{q_\infty} - \frac{p_\infty}{q_\infty} \right) \; \frac{dx}{c} = \int_0^c \left[ -\left( \frac{p_u - p_\infty}{q_\infty} \right) + \left( \frac{p_l - p_\infty}{q_\infty} \right) \right] \; \frac{dx}{c}$$

$$C_n = \int_0^c \left( -C_{p_u} + C_{p_l} \right) \; \frac{dx}{c}$$

$$C_n = \int_0^c \left( C_{p_l} - C_{p_u} \right) \; \frac{dx}{c} \tag{7}$$

Similar derivations are performed for the axial force coefficient and the moment coefficient.

**Axial force coefficient:**

$$C_a = -\int_{LE}^{TE} \frac{p_u}{q_\infty} \sin\theta \; d\left(\frac{S_u}{c}\right) + \int_{LE}^{TE} \frac{p_l}{q_\infty} \sin\theta \; d\left(\frac{S_l}{c}\right) = \int_{LE}^{TE} \left( -\frac{p_u}{q_\infty} + \frac{p_l}{q_\infty} \right) \; \frac{dy}{c}$$

$$C_a = \int_{LE}^{TE} \left( -\frac{p_u}{q_\infty} + \frac{p_l}{q_\infty} + \frac{p_\infty}{q_\infty} - \frac{p_\infty}{q_\infty} \right) \; \frac{dy}{c} = \int_{LE}^{TE} \left[ -\left( \frac{p_u - p_\infty}{q_\infty} \right) + \left( \frac{p_l - p_\infty}{q_\infty} \right) \right] \; \frac{dy}{c}$$

$$C_a = \int_{LE}^{TE} \left( C_{p_l} - C_{p_u} \right) \; \frac{dy}{c} \tag{8}$$

**Moment coefficient:**

$$C_{m_{LE}} = \int_{LE}^{TE} \frac{p_u}{q_\infty} \cos\theta \ \frac{x}{c} \ d\left(\frac{S_u}{c}\right) + \int_{LE}^{TE} -\frac{p_u}{q_\infty} \sin\theta \ \frac{y}{c} \ d\left(\frac{S_u}{c}\right) + \int_{LE}^{TE} -\frac{p_l}{q_\infty} \cos\theta \ \frac{x}{c} \ d\left(\frac{S_l}{c}\right) + \int_{LE}^{TE} \frac{p_l}{q_\infty} \sin\theta \ \frac{y}{c} \ d\left(\frac{S_l}{c}\right)$$

$$C_{m_{LE}} = \int_0^c \frac{p_u}{q_\infty} \frac{x}{c} \ \frac{dx}{c} + \int_{LE}^{TE} -\frac{p_u}{q_\infty} \frac{y}{c} \ \frac{dy}{c} + \int_0^c -\frac{p_l}{q_\infty} \frac{x}{c} \ \frac{dx}{c} + \int_{LE}^{TE} \frac{p_l}{q_\infty} \frac{y}{c} \ \frac{dy}{c}$$

$$C_{m_{LE}} = \int_0^c \left( \frac{p_u}{q_\infty} - \frac{p_l}{q_\infty} + \frac{p_\infty}{q_\infty} - \frac{p_\infty}{q_\infty} \right) \frac{x}{c} \ \frac{dx}{c} + \int_{LE}^{TE} \left( \frac{p_l}{q_\infty} - \frac{p_u}{q_\infty} + \frac{p_\infty}{q_\infty} - \frac{p_\infty}{q_\infty} \right) \frac{y}{c} \ \frac{dy}{c}$$

$$C_{m_{LE}} = \int_0^c \left[ \left( \frac{p_u - p_\infty}{q_\infty} \right) - \left( \frac{p_l - p_\infty}{q_\infty} \right) \right] \frac{x}{c} \ \frac{dx}{c} + \int_{LE}^{TE} \left[ \left( \frac{p_l - p_\infty}{q_\infty} \right) - \left( \frac{p_u - p_\infty}{q_\infty} \right) \right] \frac{y}{c} \ \frac{dy}{c}$$

$$C_{m_{LE}} = \int_0^c \left( C_{p_u} - C_{p_l} \right) \frac{x}{c} \ \frac{dx}{c} + \int_{LE}^{TE} \left( C_{p_l} - C_{p_u} \right) \frac{y}{c} \ \frac{dy}{c} \qquad (9)$$

### 2.5. Lift, Drag and Quarter-Chord Moment Coefficients

The lift, drag and quarter-chord moment coefficients are important parameters for an airfoil. The lift on an airfoil acts perpendicular to the freestream air velocity, while the drag acts parallel to the freestream. The angle between the chord line and the freestream velocity is called the angle of attack. The quarter-chord moment acts about the position located one-quarter of the chord length from the airfoil leading edge. These parameters are illustrated in Figure 5.

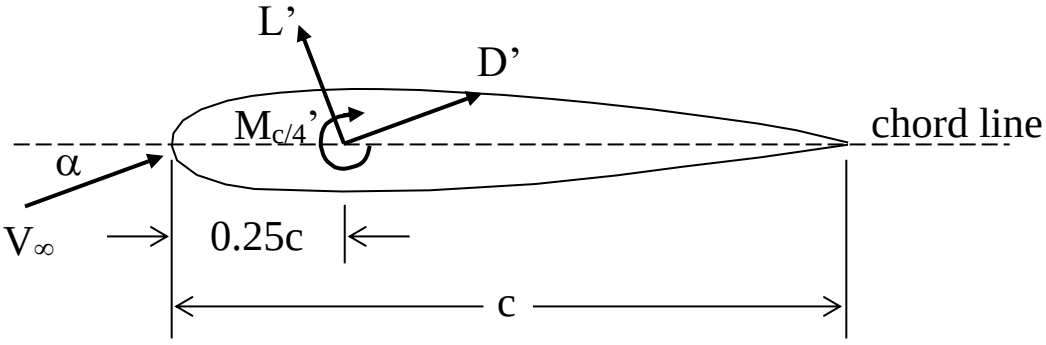


**Figure 5. Lift, drag, and 1/4 chord moment.**

The lift, drag and quarter-chord moment coefficients are defined as,

$$C_l = \frac{L'}{q_\infty c} \qquad C_d = \frac{D'}{q_\infty c} \qquad C_{m_{c/4}} = \frac{M'_{c/4}}{q_\infty c^2} \qquad (10)$$

where $L'$, $D'$ and $M'_{c/4}$ are the forces and moment per unit span.

The normal and axial force coefficients act normal and parallel to the chord line. The lift and drag coefficients act normal and parallel to the freestream velocity. Since the freestream only differs from the chord line by the angle of attack, the normal and axial forces can be used to determine the airfoil lift and drag as given by

$$\begin{aligned} C_l &= C_n \cos\alpha - C_a \sin\alpha \\ C_d &= C_n \sin\alpha + C_a \cos\alpha \end{aligned} \tag{11}$$

Note that the drag calculated from the pressure distribution only represents a small portion of the total drag for aerodynamic bodies at modest angles of attack since the drag due to the shear stress (skin friction drag), represents the majority of the drag at those conditions.

Similarly, the leading-edge moment coefficient and the lift coefficient can be used to calculate the quarter-chord moment coefficient which is given by

$$C_{m_{c/4}} = C_{m_{LE}} + \tfrac{1}{4} C_l \tag{12}$$

**2.6. Discretization of Equations**

In order to apply the above force and moment equations to an actual airfoil model with a limited number of pressure taps, the equations must be discretized since pressures are available only at the discrete locations of the taps. This is accomplished by the Trapezoidal Rule, in which the integral of a function (or the area under the curve) is approximated by the summation of numerous trapezoidal areas. For the function *f(z)*, the integral *I* is approximated as,

$$I = \tfrac{1}{2}(f_0+f_1)(z_1-z_0) + \tfrac{1}{2}(f_1+f_2)(z_2-z_1) + \ldots + \tfrac{1}{2}(f_{n-1}+f_n)(z_n-z_{n-1}) \tag{13}$$

Thus the discrete normal and axial force equations are,

$$\begin{aligned} C_n &= \sum_{i=TE}^{\#taps} \frac{1}{2}\left(C_{p_i} + C_{p_{i+1}}\right)\left(\frac{x_{i+1}}{c} - \frac{x_i}{c}\right) \\ C_a &= -\sum_{i=TE}^{\#taps} \frac{1}{2}\left(C_{p_i} + C_{p_{i+1}}\right)\left(\frac{y_{i+1}}{c} - \frac{y_i}{c}\right) \end{aligned} \tag{14}$$

where the summation begins at the airfoil trailing-edge position, continues along the upper surface toward the leading edge, curves around to the lower surface and returns to the trailing edge.

The discrete leading-edge moment equation is,

$$C_{m_{LE}} = \sum_{i=TE}^{\#taps} \frac{1}{2}\left(C_{p_i}\frac{x_i}{c} + C_{p_{i+1}}\frac{x_{i+1}}{c}\right)\left(\frac{x_i}{c} - \frac{x_{i+1}}{c}\right) + \sum_{i=TE}^{\#taps} \frac{1}{2}\left(C_{p_i}\frac{y_i}{c} + C_{p_{i+1}}\frac{y_{i+1}}{c}\right)\left(\frac{y_i}{c} - \frac{y_{i+1}}{c}\right) \tag{15}$$

The lift, drag and quarter-chord moment coefficients are easily calculated from the above expressions.

### 2.7. Reynolds Number and Mach Number

For a body of given shape and orientation with a characteristic length scale ($l$) in a fluid of velocity ($V$), the force ($F$) experienced by the body from the motion through the fluid is,

$$F = f(\rho, V, l, \mu, a) \tag{16}$$

where $\rho$ = density of the fluid [slug/ft$^3$; kg/m$^3$]
$\mu$ = coefficient of viscosity for air [slug/ft/sec; kg/m/sec]
$a$ = speed of sound [ft/sec; m/sec]

The force coefficient for a body of given shape and orientation is a function of two dimensionless parameters, the Reynolds number and Mach number.

The Reynolds number is the ratio of the inertial forces to the viscous forces and is defined as

$$\mathrm{Re} = \frac{\rho V l}{\mu} = \frac{\rho V c}{\mu} \tag{17}$$

where $\rho$ = density of air [slug/ft$^3$; kg/m$^3$]
$V$ = test-section airspeed [ft/sec; m/sec]
$c$ = airfoil chord [ft; m]
$\mu$ = coefficient of viscosity for air [slug/ft/sec; kg/m/sec]

It should be noted that the viscosity is a function of the temperature and can be obtained from tables or by using Sutherland's law, a common equation found in most fluid dynamics texts. For subsonic airfoil studies, the characteristic velocity is most often the freestream velocity in the test section. The characteristic length scale is usually the airfoil chord length (as given above).

The Mach number is the ratio of the local fluid speed to the local speed of sound and is defined as,

$$M = \frac{V}{a} \tag{18}$$

where $V$ = test-section airspeed [ft/sec; m/sec]
$a$ = speed of sound [ft/sec; m/sec] = $(\gamma RT)^{1/2}$

## 3. LABORATORY EQUIPMENT

The primary pieces of equipment and instrumentation used in this experiment are listed below.

Aerolab low-speed wind tunnel
Clark Y airfoil model
Pressure Systems Incorporated (PSI) NetScanner pressure system
Digital Barometer/Thermometer
Personal computer with LabVIEW software
Tufts

### 3.1. Aerolab Low-Speed Wind Tunnel

The wind tunnel is located in Room 18D of Talbot Laboratory. It is an Eiffel-type, open-return tunnel. Air is drawn into the elliptical inlet, through a honeycomb and screen section, and is

accelerated through the contraction into the test section. The wind tunnel air then decelerates through the diffuser section and into the fan. The air is discharged into the atmosphere. A sketch of the tunnel is shown in Figure 6.

The wind tunnel is made up of the following components:

1. **Bellmouth and Flow-Conditioning Section**: The air from the room enters the bellmouth and is delivered to the flow conditioning section. A precision aluminum honeycomb and three graduated, high-porosity screens, mounted and tensioned in extruded aluminum frames, provide the flow conditioning.
2. **Static Pressure Ring**: The static pressure ring is a copper tube manifold that connects four static pressure taps (one orifice on each wall). The static pressure ring is located downstream of the contraction section and just upstream of the test section. By grouping

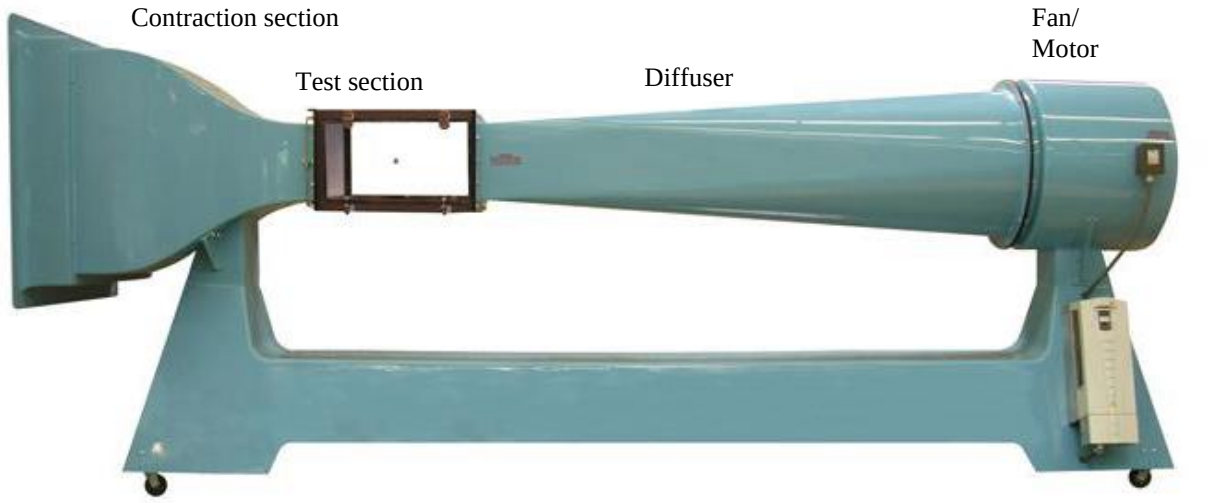


**Figure 6. Schematic of Aerolab low-speed wind tunnel. [1]**

the static pressure taps in this manner, the pressure will represent the average static pressure at all four walls. The static pressure ring is used to monitor the wind tunnel dynamic pressure (or speed) when running an experiment by assuming that the stagnation pressure is equal to the atmospheric pressure. Because there are losses at the entrance to the contraction, mostly due to the honeycomb flow straightener and turbulence-reducing screens in the flow-conditioning section, a calibration factor found in the previous experiment is applied to this measured pressure difference ($P_{atm} - P_{static,ring}$), so the actual dynamic pressure in the test section can be calculated. Note also that the static pressure ring is used as a reference pressure for all the pressures on the airfoil.

3. **Contraction Section**: The air accelerates in the contraction section to the test-section speed. This acceleration also reduces the relative intensity of turbulent eddies. The contraction has a 9.5:1 area ratio, with a symmetrical cross section and analytically developed contours.
4. **Test Section**: This in the location of the highest flow velocity and is where the testing is done. The interior dimensions of the test section are: length, 24”; width, 12”; height, 12”.
5. **Diffuser**: The diffuser allows the test-section flow to decelerate without flow separation from the walls. A wire mesh safety grid is provided at the downstream end of the primary diffuser.

6. **Fan and Drive Motor**: An axial-flow fan assembly is used. The fan is direct driven by a 10 HP, variable speed, AC induction motor. A transistor-type variable frequency drive regulates the RPM which is set by a frequency input. A speed control station, located at the upstream end of the diffuser, regulates the test-section velocity by varying the frequency of the AC power supplied to the motor. The inverter is set by either a keypad, shown in Figure 7, or RS-232 serial input from a computer.

### 3.2. 3.5-inch Chord Clark Y14 Airfoil Model

The model is a Clark Y14 airfoil of 3.5-inch chord with a thickness of 14% of the chord (compared to the 11.7% thickness of the normal Clark Y airfoil). The cross-section is illustrated in Figure 8. There are 18 pressure taps located around the model, 9 on the upper surface, 8 on the lower surface and 1 at the leading edge. Figure 8 shows the chord-wise tap distribution. All tap positions are depicted in inches. Although there is no pressure tap at the thin trailing edge of the profile, the pressure there is approximated by averaging the last taps on the upper and lower surfaces together. The airfoil is mounted on the floor of the wind tunnel (Figure 9) on a rotation base, which can be used to set the angle-of-attack using the marks on the bottom wall (viewed inside the test section) and lever located outside the wind tunnel.


**Figure 7. Frequency control keypad to regulate tunnel speed.**

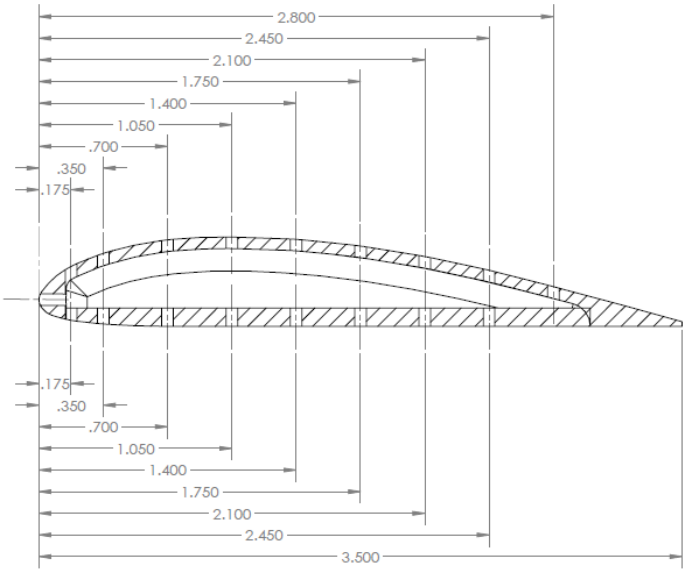


**Figure 8. Clark Y14 airfoil cross-section. [1]**

### 3.3. PSI NetScanner Pressure System

The pressure measurement system consists of three NetScanner System Intelligent Pressure Scanner (model 9016) modules (Figure 10). Each of these modules has integral pressure transducers and a pneumatic calibration manifold. There are two 1-psid modules, which can measure maximum differential pressures of 1.0 psid, with an accuracy of 0.1% of the full-scale value. A differential pressure measurement is the pressure difference between two sources.

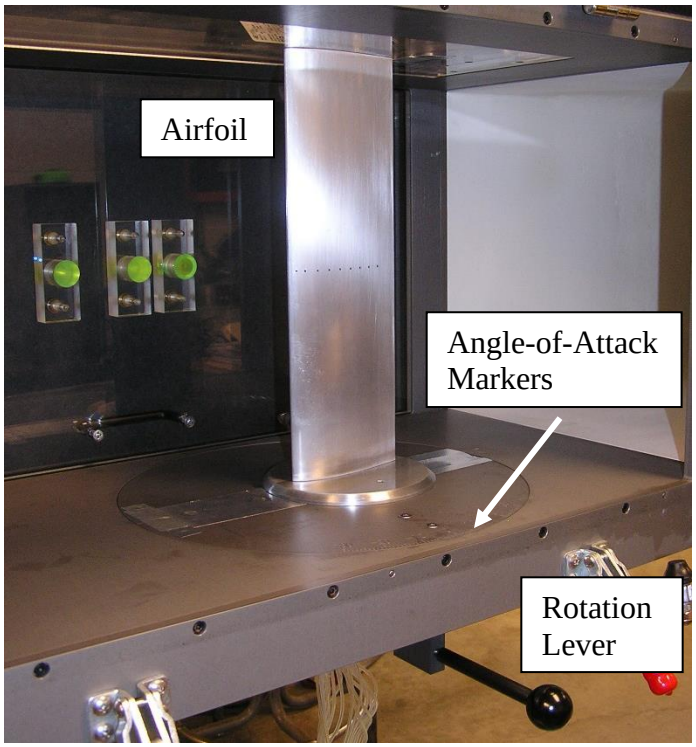


**Figure 9. Clark Y14 airfoil mounted on the floor of the wind tunnel.**


**Figure 10. PSI NetScanner pressure system.**

Each module consists of 16 ports and a reference port. The pressure differences between each of the 16 ports and the reference pressure produce the 16 differential pressures. For the current experiment, the static pressure ring is connected to the reference ports of both modules and one of the ports is left open to the atmosphere so that the dynamic pressure in the test section can be determined using the correction factor determined in the previous calibration lab. Pressure data are acquired by the NetScanner system and are transferred to the attached computer by a LabVIEW program with the front panel shown in Figure 11. The NetScanner system occasionally needs to be re-zeroed. This is also accomplished through the LabVIEW program by pressing the [**Tare PSI Modules]** button on the front panel.

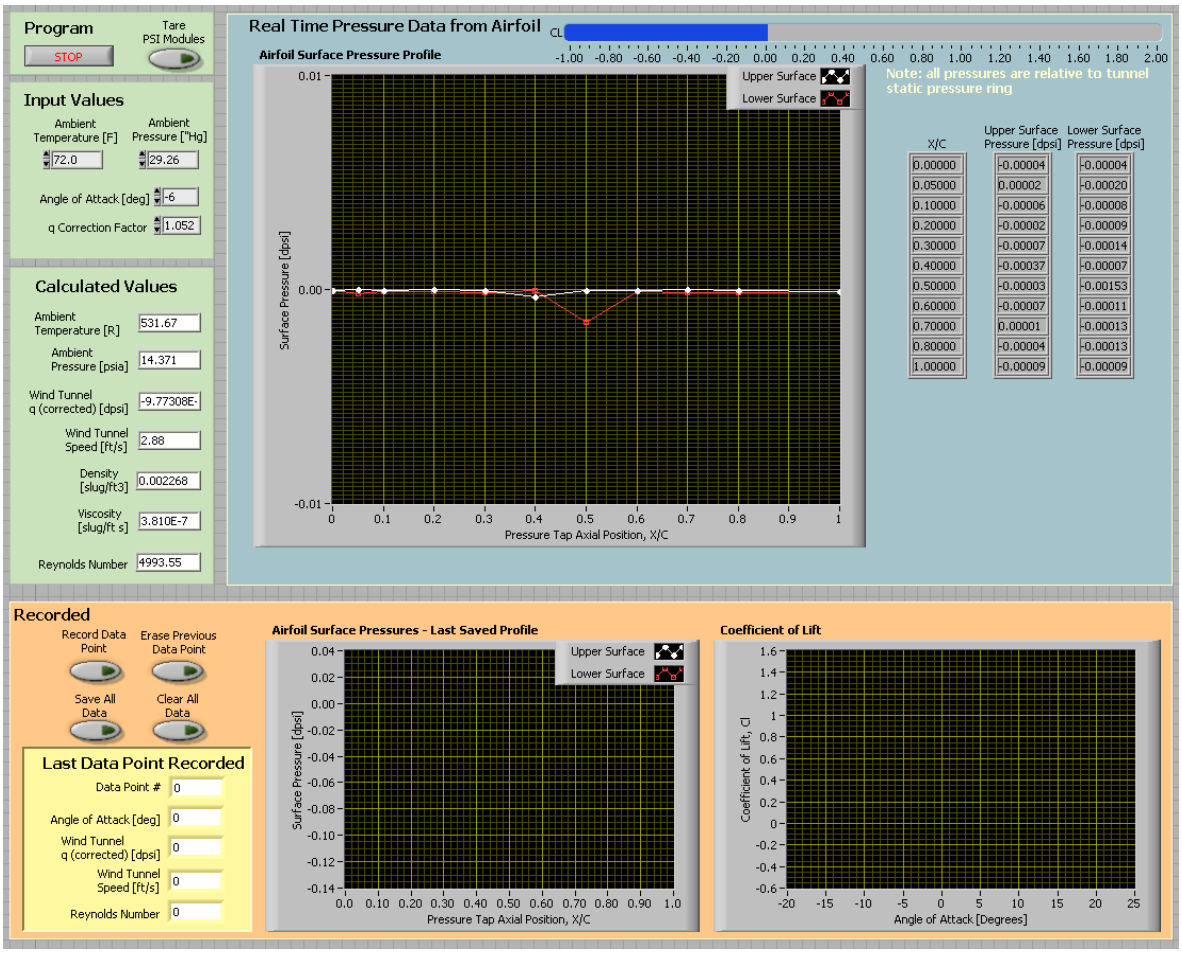


**Figure 11. Front panel of LabVIEW program.**

### 3.4. Compact Digital Barometer

The compact digital barometer (Model 4195) made by Control Company is NIST traceable and is used to measure the atmospheric pressure and temperature in the laboratory. The barometer has an accuracy of ± 0.148 in Hg, and the temperature is measured with an accuracy of ±1.8℉. It can display either English or SI units. http://www.control3.com/4197p.htm

### 3.5. Tufts

The tufts used in this experiment are made from embroidery thread and are approximately 1.5" long. A little super glue on the ends keeps the threads from fraying. As the air flows over the surface, the tufts align with the local direction of the streamlines due to the imposed shear stress.

## 4. PROCEDURE

Please follow each of the outlined steps closely. Words denoted in bold (e.g., **[Start]**) indicate physical buttons on the frequency control keypad, computer keyboard, or radio buttons on the computer screen. Radio buttons are activated by pressing the left mouse button while the cursor is placed over the radio button.

### 4.1. Familiarization with Equipment

Locate each of the following pieces of equipment in the laboratory:

1. Locate the airfoil in the test section and notice how it is mounted.
2. Locate the airfoil pressure taps and notice how the pressure lines are connected to the PSI system modules. *Make sure all of the pressure tubes are unobstructed and are not crimped.*
3. Locate the angle-of-attack indicator and verify how to adjust the angle before starting the tunnel.
4. Locate the tunnel frequency controller keypad (Figure 7) and make sure the system is in local mode. This is shown in the upper left hand corner of the screen by the **LOC** abbreviation. If it does not show **LOC**, simply press the **[LOC/REM]** button on the controller. This allows local or manual control of the frequency, rather than remote control by the computer. The **[START]** button starts the motor. The up and down arrows on the controller allow the angular speed **(RPM)** of the motor to be adjusted. The set point for the motor speed is shown in RPM in the upper right hand corner of the display. The rest of the display will show the frequency input to the motor, as well as the amperage it is drawing from the controller. The **[STOP]** button will stop the motor, but the last RPM setting will still be saved for the next start-up.

### 4.2. Angle-of-Attack Pressure Survey

1. Run the AE 460 shortcut from the computer desktop by double-clicking on the **[AE 460 Airfoil Lab]** icon.
2. Under the **Input Values** block, you will be entering atmospheric data for the runs for the day of the test and for each run setting. Read and record the barometric pressure and the atmospheric temperature. Enter the atmospheric values, in inches Hg and degrees Fahrenheit, on your data sheet and type the values into the computer interface (left click the box and type in the appropriate value) in the boxes labeled **Ambient Pressure [Hg"]** and **Ambient Temperature [F]**, respectively.
3. Enter the value of the dynamic pressure correction factor into the numerical control labeled **[q Correction Factor]**, which was determined from the calibration measurements in the previous lab. Write this value on the data sheet also.
4. With the tunnel off, left click the **[Tare PSI Module]** button (upper left corner of the program). This re-zeroes all the transducers in the PSI NetScanner system.
5. Verify that the airfoil is at zero angle-of-attack and secure in the wind tunnel.
6. Verify that the RPM is set to zero on the frequency control pad and press the **[START]** button.
7. Adjust the tunnel speed input frequency with the up **[⇑]** and down **[⇓]** arrow buttons on the keypad, setting the frequency so that the freestream velocity in the wind tunnel is equal to 90 ft/s. The angular velocity of the fan will be approximately 1100 RPM to obtain this velocity (**Do not exceed 1500 RPM throughout the test**).
8. Adjust the angle-of-attack of the airfoil to the first point, which is -6 degrees. You will need to give the pressure transducers time to equilibrate, and iterate the frequency input to obtain a

value close (within ± 2 ft/s) to the desired velocity as you change the angle-of-attack of the airfoil.

9. Once the desired freestream velocity is achieved, enter the angle of attack into the numerical control on the computer program **Angle of Attack [deg]**. Note that the surface pressure data are presented in real-time on the upper graph and numerical indicators to the right of it.
10. **As the angle of attack is changed, the fan angular speed may need to be adjusted slightly since the blockage of the model varies and causes the tunnel freestream velocity to change slightly.** Once the desired velocity is achieved, press the **[Record Data Point]** button on the computer interface to record and store all of the airfoil pressure measurements through the PSI system along with the other parameters.
11. On the data sheet, record the freestream dynamic pressure (which has been automatically corrected in the program) along with the velocity and Reynolds number of the recorded point from the **[Last Data Point Recorded]** dialog box.
12. Observe the behavior of the flow visualization tufts. Take some notes regarding them, or take a photograph (using one of your phones). In your report, do not present and discuss all of your tuft images. Only use enough of them to describe the key flow characteristics as you increase angle of attack. Remember to consider both the upper and lower surfaces.
13. Obtain an angle-of-attack sweep repeating steps 8-12. Starting at $\alpha = -6^o$, increase the angle of attack and take data at every 2 degrees until passing stall (up to ~$26^o$). Stall can be observed by the coefficient of lift graph (lower right of the front panel). Take note of the behavior of the tufts as you change the angle-of-attack (write down any observations in the space provided which will aid you in the flow visualizations to follow). Continue to take data decreasing the angle of attack back to $-6^o$. Obverse and note and differences between the lift coefficient when increasing and decreasing the angle of attack. Differences might be evident near stall, and this effect is referred to as hysteresis. If hysteresis is observed, comment on the observations and theorize why it might occur in the lab report. **When changing the angle of attack, be sure to grip the lever firmly since it will want to rotate at high angles-of-attack.** Also maintain the velocity at each angle-of-attack by slightly adjusting the input fan speed to the wind tunnel motor. Do not forget to enter the value of the angle-of-attack before you press the **[Record Data Point]** button.
14. After the last point is recorded, observe the coefficient of lift versus angle-of-attack plot and write down the angle of attack for the maximum coefficient of lift and where the airfoil stalls (lift drops off most sharply). Press the **[Save All Data]** button, which will bring up a dialog panel and allow you to save your data file. You should save the file to your network folder which usually appears as the **H:** drive in the file dialog menu. It is suggested that you use a file name with a **.csv** suffix, which will help programs recognize that the ASCII text file has comma separated variables. Write down the name that you use.
15. Return the angle-of-attack of the airfoil to zero and again adjust the velocity to 100 ft/s.
16. Shut down the tunnel by pressing the **[STOP]** button.

### 4.3. Output Datafile Format

The lab data are output to the file in rows of data. There is a row of data for each angle-of-attack acquisition. The data are organized in rows as follows:

DataPoint #:
AOA (deg): ***angle of attack***
Q_WT corrected (dpsi): ***corrected wind tunnel freestream dynamic pressure***
q_corr_fac: ***q correction factor***
AmbTemp (Rankine):
AmbPress (psi):
Reynolds Num:
x/c y/c p(psid) ***the tap position x/c and y/c values are given in the header with the pressure data for each angle of attack given below them. The values start from the trailing edge and go around the top surface to the leading edge and then back along the bottom surface.***

Note: *p(psid)* is defined as the static differential pressure on the model surface ($\Delta p_{measured}$) as described and given previously in the equations above. Also, "*q corrected*" is the dynamic pressure of the wind tunnel test section with the correction factor already applied automatically in the program [i.e. q_WT corrected*(q_corr_fac)].

## 5. DATA PROCESSING AND PRESENTATION

Using the data obtained during the experiment, perform the following calculations and answer the corresponding questions.

### Angle-of-Attack Pressure Survey Results

1. Tabulate the following reduced data: $C_n$, $C_a$, $C_{mLEx}$, $C_{mLEy}$, $C_l$, and $C_{mc/4}$ for each angle of attack. Comment on any trends you observe.

2. Tabulate the corrected dynamic pressure, velocity, Reynolds number and Mach number for each angle of attack. Depending on the viscosity value you use, the Reynolds number may differ slightly from the values in the output file. Comment on any trends you observe.

3. Plot the pressure coefficient versus *x/c* for the angles-of-attack -4, 0, 4, 8, 12 degrees all on the same graph. Recall that it is traditional to plot negative pressures in the upward direction of the graph *y*-axis and the positive pressures down. Comment on how the pressure distribution changes with increasing angle of attack. Compare the pressure distribution for the upper and lower surfaces at zero angle of attack (i.e., are they the same or different and why).

4. Plot the pressure coefficient versus *x/c* for the angles-of-attack 8, 16, 20, 24 degrees all on the same graph. Recall that it is traditional to plot the negative pressures in the upward direction of the graph *y*-axis and the positive pressures down. Comment on how the pressure distribution changes with increasing angle of attack, particularly as the airfoil starts to stall.

5. Plot the lift coefficient versus angle of attack. Discuss and comment on any trends you observe and possible causes for those trends.

6. Plot the quarter-chord pitching-moment coefficient versus angle of attack and comment on any trends you observe.

7. Compare your results (i.e., lift, pitching moment, etc.) to a few other airfoil types (two or three) which you can easily find in the literature or on the internet. Be sure to indicate the nomenclature (i.e., name or NACA designation) for the airfoils you select and reference where you obtained the data. Also, make sure one of the airfoils you compare to is a symmetric airfoil. Comment and give possible reasons for any similarities or differences you observe.

**Surface Flow Visualization (Tufts) Results**

8. Present your tuft flow visualization results (images, pressure profiles, lift and moment data) in a clear and concise manner. The goal of this section is to describe the differences between the flow near the surface when the airfoil is at zero angle-of-attack and changes that are observed as the airfoil stalls. Also, you should attempt to reinforce your description and interpretation combined with information obtained from the pressure profiles, lift, and moment data calculated for the angles-of-attack investigated with the tuft flow visualizations. This is an open-ended question graded on your ability to synthesize and present your data in a clear, concise manner drawing correct conclusions.

Show example calculations in the appendix and be sure to comment on the uncertainty of your measurements (a detailed uncertainty analysis is not necessary for this lab). Include a copy of the raw data sheet, which was handwritten during the laboratory.

## REFERENCES

1. Drawing provided by Dan Rodgerson of Aerolab, "Base Pressure Wing," www.aerolab.com, 2011.

**Data Table for Airfoil Pressure Distribution Experiment**

Name _____

Section/Group _____ Date _____

Ambient Pressure [“Hg] _____

Ambient Temperature (°F) _____

q Correction Factor _____

| Data Point | α [deg] | Wind Tunnel q (corrected) [dpsi] | Velocity [ft/sec] | Reynolds Number |
|---|---|---|---|---|
| 1 | | | | |
| 2 | | | | |
| 3 | | | | |
| 4 | | | | |
| 5 | | | | |
| 6 | | | | |
| 7 | | | | |
| 8 | | | | |
| 9 | | | | |
| 10 | | | | |
| 11 | | | | |
| 12 | | | | |
| 13 | | | | |
| 14 | | | | |
| 15 | | | | |
| 16 | | | | |
| 17 | | | | |
| 18 | | | | |
| 19 | | | | |
| 20 | | | | |

Angle-of-attack for the maximum coefficient of lift_____

Angle-of-attack for stall (may be given as a range)_____

Flow Visualization Data

| Data Point | α [deg] | Wind Tunnel q (corrected) [dpsi] | Velocity [ft/sec] | Reynolds Number |
|---|---|---|---|---|
| 1 | | | | |
| 2 | | | | |
| 3 | | | | |
| 4 | | | | |
| 5 | | | | |
| 6 | | | | |
| 7 | | | | |

Notes and Observations: